arXiv:1602.07823v1 [physics.optics] 25 Feb 2016

Generation of nonlinear vortex precursors

Yue-Yue Chen,[1,2] Xun-Li Feng,[3] and Chengpu Liu[1,*]

[1] *State Key Laboratory of High Field Laser Physics, Shanghai Institute of Optics and Fine Mechanics, Chinese Academy of Sciences, Shanghai 201800, China*

[2] *University of Chinese Academy of Sciences, Beijing 100039, China*

[3] *Department of Physics, Shanghai Normal University, Shanghai 200234, China*

(Date textdate; Received textdate; Revised textdate; Accepted textdate; Published textdate)

We numerically study the propagation of a few-cycle pulse carrying orbital angular momentum (OAM) through a dense atomic system. Nonlinear precursors consisting of high-order vortex harmonics are generated in the transmitted field due to ultrafast Bloch oscillation. The nonlinear precursors survive to propagation effects and are well separated with the main pulse, which provide a straightforward way of measuring precursors. By the virtue of carrying high-order OAM, the obtained vortex precursors as information carriers have potential applications in optical information and communication fields where controllable loss, large information-carrying capacity and high speed communication are required.

PACS numbers: 42.65.Ky, 42.65.Re, 42.25.Bs, 42.50.Tx, 42.50.Gy

More than one century ago, the concept of optical precursors [1] emerged from the seminal works of Sommerfeld [2] and Brillouin [3, 4] on asymptotic description of ultrawideband dispersive pulse propagation in linear dielectrics. This description is derived from the exact Fourier-Laplace integral representation of the propagated linearly polarized plane wave field [5] and approximating the material system as a collection of linear oscillators [6]. To observe precursors, considerable theoretical [7–11] and experimental [12–15] studies on optical precursors have been done over years. However, many initial works focused on an opaque medium with single or multiple Lorentz absorption lines, where the main signal is either absorbed or cannot be well separated from precursors. This provokes controversies about the existence of precursors [16, 17].

Recently, it has been reported that the precursors also exist in nonlinear interactions regime [18–20]. Ding *et al.* observed optical precursors, which consist of the high-frequency components of the signal pulse, in four-wave mixing based on a cold-atom gas [18]. Palombini *et al.* studied the effects of a nonlinear medium response on precursor formation using the split-step Fourier method [20]. In both cases, the nonlinear precursors are obtained with the main pulse absorbed by the medium. A scheme to obtain nonlinear precursors in a two-level system with rotating-wave approximation (RWA) and slowly varying envelope approximations (SVEA) is proposed, where the precursors are well separated with main pulse [19]. However, for the few-cycle physics, the standard approximations used in traditional nonlinear optics are no longer appropriate [21]. Thus, the full wave Maxwell-Bloch (MB) equations without SVEA and RWA need to be solved.

On the other hand, light beams can exhibit helical wave fronts [22, 23]. High-order optical vortex beam has many potential applications such as generating Multi-dimensional entanglement to support efficient use of communication channels in quantum cryptography [24], and photoexciting atomic levels without the restriction of standard dipolar selection rules [25, 26]. Recently, schemes using gas [27] and plasma [28] as mode converters to increase the OAM of a beam charge have been proposed. Their schemes conflate high-order harmonics generation (HHG) and OAM, imprinting the phase twist to the fundamental field instead of the short-wavelength radiation directly. However, these schemes either require extremely intense ($\sim 10^{15}\mathrm{W/cm^2}$) or even relativistic laser pulses ($\sim 10^{22}\mathrm{W/cm^2}$), where damage thresholds of the nonlinear medium have to be considered, or are restricted to an ultrathin medium ($\sim 1\mu\mathrm{m}$), where propagation effect are ignored.

In this paper, we presents a scheme to generate nonlinear precursors consisting of high-order vortex harmonics in relatively low energy physics, where the propagation effects are considered. A dense two-level atomic medium is used as a mode converter to manipulate the OAM of a few-cycle helical pulse. Interestingly, nonlinear precursors consisting of high-order vortex harmonics appear in the front of the fundamental field. Compared with that obtained in reflected field [28], the high-order vortex harmonics existed in the precursors are instinctively separated from the fundamental mode, sparing the necessity of a filter to observe the harmonics. Therefore, our proposal generates high-order vortex harmonics with merits of precursors, relaxes the requirement of extremely intense pulse for ionization or plasma generation, and takes propagation effects into consideration. Using high-order vortex precursors as information carriers in quantum information can favor the realization of high-speed communication, enhance the efficiency of communication channels, and improve the robustness to resonant absorption loss.

*Electronic address: chpliu@siom.ac.cn

A few-cycle Laguerre-Gaussian (LG) laser pulse propagates along z in vacuum and is incident on a dense two-level atomic medium. Assuming the driving pulse is linearly polarized along x, the incident pulse takes the form $E(t=0,z) = E_{lp}\cos[\omega_p(z-z_0)/c]\,\mathrm{sech}[1.76(z-z_0)/(c\tau_p)]\hat{e}_x$, where ω_p is the carrier frequency, τ_p the full width at half maximum of the pulse intensity envelop, $\hat{e}_x$ the unit vector in x direction. The initial position z_0 is set to be 3μm to avoid the pulse penetrating into the medium at $t=0$. The amplitude E_{lp} is defined by [29]

$$\begin{aligned} E_{lp}(t=0,z) = & \frac{E_0}{(1+\tilde{z}^2/z_R^2)^{1/2}}(\frac{r}{a(\tilde{z})})^l L_p^l(\frac{2r^2}{a^2(\tilde{z})}) \\ & \times \exp(-\frac{r^2}{a^2(\tilde{z})})\exp(-\frac{ikr^2\tilde{z}}{2(\tilde{z}^2+z_R^2)})\exp(-il\phi) \\ & \times \exp(i(2p+l+1)\tan^{-1}\frac{\tilde{z}}{z_R}), \end{aligned} \tag{1}$$

where $\tilde{z} = z - z_0$, E_0 is the peak amplitude of the incident pulse, z_R the Rayleigh range, $a(\tilde{z})$ the radius of the beam, L_p^l associated Laguerre polynomial, and the beam waist a_0 is at $z = z_0$. The characteristic helical phase profiles of optical vortices are described by $\exp(-il\phi)$ multipliers, where $l(l = 0, \pm1, \pm2...)$ is the topological charge corresponding to the mode order and ϕ the azimuthal coordinate. The integer p denotes the number of radial nodes in the mode profile. The three-dimensional Maxwell's equations in an isotropic medium take the form

$$\begin{aligned} \frac{\partial \mathbf{H}}{\partial t} &= -\frac{1}{\mu_0}\nabla\times\mathbf{E}, \\ \frac{\partial \mathbf{E}}{\partial t} &= \frac{1}{\epsilon_0}\nabla\times\mathbf{H} - \frac{1}{\epsilon_0}\frac{\partial \mathbf{P}}{\partial t}. \end{aligned} \tag{2}$$

The macroscopic polarization induced by the linearly polarized electric field is $P_x\hat{e}_x$. $P_x = Ndu$ is associate with the off-diagonal density-matrix element $\rho_{12} = (u+i\upsilon)/2$, N the density and d the dipole moment. The population inversion between the excited 2 and the ground state 1 is denoted by $w = \rho_{22} - \rho_{11}$. u, υ and w obey the following set of Bloch equations,

$$\begin{aligned} \frac{\partial u}{\partial t} &= -\gamma_2 u - \omega_0 \upsilon, \\ \frac{\partial \upsilon}{\partial t} &= -\gamma_2 \upsilon + \omega_0 u + 2\Omega w, \\ \frac{\partial w}{\partial t} &= -\gamma_1(w - w_0) - 2\Omega\upsilon. \end{aligned} \tag{3}$$

Where γ_1, γ_2 are, respectively, the population and polarization relaxation rate, ω_0 the resonant frequency, $\Omega(z,t)$ the Rabi frequency, and w_0 is the initial population difference.

The full wave MB equation can be solved by adopting Yee's finite-difference time-domain (FDTD) discretization method for the electromagnetic fields [30, 31] and the predictor-corrector method [32, 33] or the fourth order Runge-Kutta method [34] for the medium variables. The medium is initialized with $u = \upsilon = 0, w_0 = -1$. The following parameters are used to integrate the MB equations: $\omega_0 = \omega_p = 2.3\mathrm{fs}^{-1}$, $d = 2\times10^{29}\mathrm{A{*}s{*}m}$, $\gamma_1^{-1} = 1\mathrm{ps}, \gamma_2^{-1} = 0.5\mathrm{ps}, \tau_p = 5\mathrm{fs}, a_0 = 7\mu$m, medium length $L = 25\mu$m, $\Omega_0 = 1.408\mathrm{fs}^{-1}$, the corresponding pulse area is $A(z) = d/\hbar\int_{-\infty}^{\infty}E_0(z,t')dt' = \Omega_0\tau_p\pi/1.76 = 4\pi$ [35]. Defining a collective frequency parameter $\omega_c = Nd^2/\epsilon_0\hbar = 0.1\mathrm{fs}^{-1}$ to present the coupling strength between medium and field. Our simulation region is padded with perfectly matched layers that prevents back reflection from the truncated simulation region.

With the given parameters, the evolutions of a LG_{10} beam at $z = 9$ μm and 30 μm are obtained, as shown in Fig. 1. The evolution of LG_{10} beam with two lobes is quite similar with that of two out-of-phase 2π pulses [36]. Since the local delays are inversely proportional to the local Rabi frequency, each lobe of the LG_{10} beam evolves progressively into a crescent-shaped pulse, accompanying with self-focus caused by the diffraction-induced inward flow of energy from the outer rings [37, 38], as shown in Fig. 1(a). However, due to transverse effect, the crescent-shaped fields are unstable [37]. Each of them breaks up

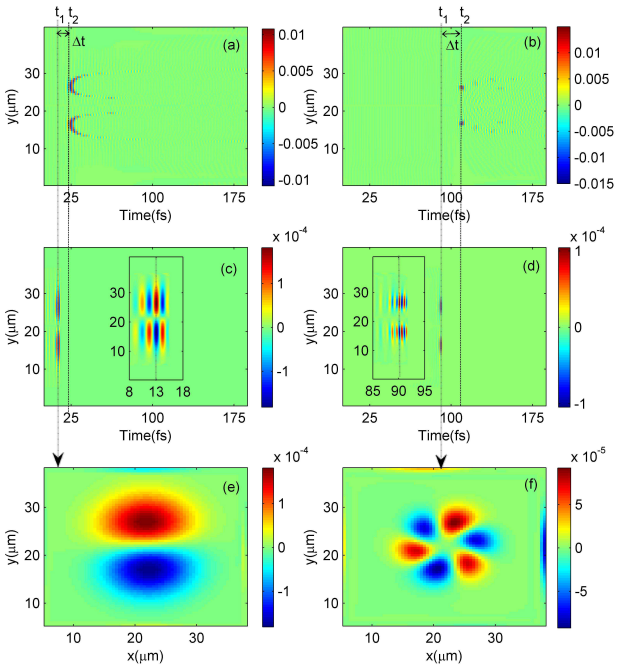

FIG. 1: (color online) (top) Time evolutions of E_x at $z_1 = 9\mu$m (left) and $z_2 = 30\mu$m (right). (middle) The corresponding evolutions of the leading part of the precursors and their enlarged view in the inserts. (bottom) The corresponding transverse distribution of E_x at t_1.

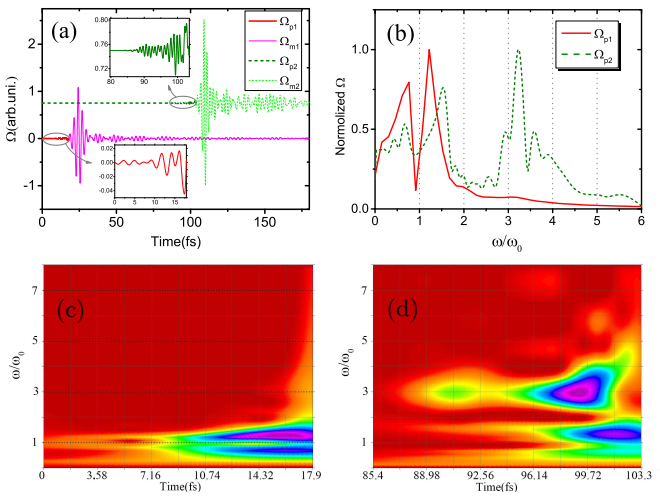

FIG. 2: (color online) The precursors (a) and their spectra (d) correspond to $z_1 = 9\mu$m (solid line) and $z_2 = 30\mu$m (dashed line), respectively, at $x = 21.5\mu$m and $y = 16.5\mu$m. The time-frequency analysis graphs of precursors correspond to z_1 (c) and z_2 (d), respectively.

into a leading 2π SIT soliton located at lobe-peak and several small-area fragments at wings. As the pulse further propagates, only the two leading 2π SIT-like solitons survived. All the small-area fragments experience energy decrease and vanish at a large distance, as shown in Fig. 1(b).

More importantly, precursors ahead of the main pulse are generated during the propagation. The precursors consist of off-resonant frequency components and propagate with the speed of light in vacuum, while the main pulse is delayed by the resonant medium. The leading part of the precursors are shown in Figs. 1(c) and 1(d). At the beginning of the propagation ($z = 9\mu$m), the electric field of precursors in longitudinal plan is similar with that of incident pulse, in terms of the beam diameter and carrier frequency, as shown in Fig. 1(c). In addition, the transverse plane of the precursors in Fig. 1(e) shows the LG_{10}-like mode as the driving pulse. Later, at $z = 30\mu$m, the precursors have a much smaller beam diameter and a much higher carrier frequency than that at the beginning. The decrease of beam diameter is caused by self-focusing. The corresponding transverse electric field in Fig. 1(f) shows a LG_{30}-like mode. Meanwhile, the distance between the leading of the precursors and the main pulses, i.e. $\Delta t = t_2 - t_1$, increases along the propagation path, which confirms the theory that precursors propagate faster than main pulse.

To have a overall understanding of precursors, the electric fields at z_1 and z_2 are obtained. As shown in Fig. 2(a), precursors (thick line) emerge in front of the main pulse (thin line) and evolve to a structure with fast oscillations. The spectra in Fig. 2(b) show that dominate frequency components of the precursors change from near-resonant frequency to third harmonic. To further investigate the frequency changes of precursors induced by propagation, we performed time-frequency analysis to z_1 and z_2, respectively. For z_1, where the interaction length is relatively short, the precursors are linear. These linear precursors contain high- and low-frequency components corresponding to Sommerfeld and Brillouin precursors, respectively, as shown in Fig. 2(c). Then, odd harmonics are generated but barely separated with main pulse. Since the atoms cannot respond quickly to rapid changes in electric field corresponding to odd harmonics, the high-frequency components pass through the atoms without any delay and are gradually separated from the delayed main pulse. As shown in Fig. 2(c), for $z_2 = 30\mu$m, the third harmonic is well separated with main pulse and become the dominant frequency components of precursors. In this case, the linear precursors becomes nonlinear. Thus, the transformation of linear to nonlinear precursors occurs along propagation path.

Since the nonlinear precursors are separated from the main pulse by nature, their vortex information can be obtained without the necessary of filtering the fundamental field. It can be seen from Figs. 3(e)-3(f) that the changes of the electric field distributions within one loop show clearly helical feature. The distance of rotating one loop of E_x is approximately $\lambda_3 = 0.27\mu$m, which is equal to the wavelength of the third harmonics $\lambda_0/3$. The corresponding three-dimensional temporal evolution of the field in Fig. 3(a) is shown in Fig. 3(b), where the helical structure of third harmonic field can be seen clearly. Thus, third-order vortex precursors appear at the front of the main pulse.

Moreover, as showed in Fig. 2 (d), higher-order harmonics coexist with third harmonic in nonlinear precursors. The transverse distributions of the third, fifth, sev-

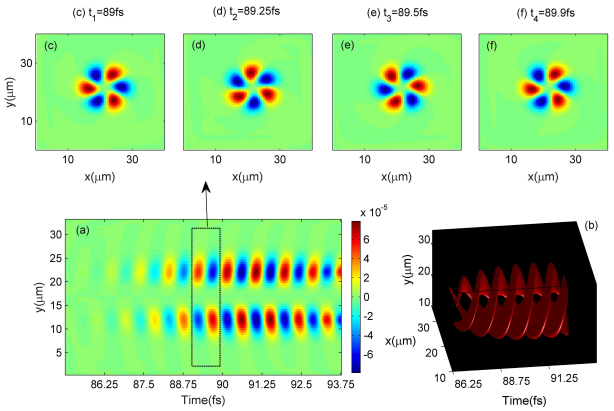

FIG. 3: (color online) (a) The time evolution of E_x at $z_3 = 30\mu$m during [85fs, 93.75fs]. (b) The corresponding 3D spatial distribution of E_x. (c-f) The distribution of E_x in $x - y$ plan during the time of rotating one loop.

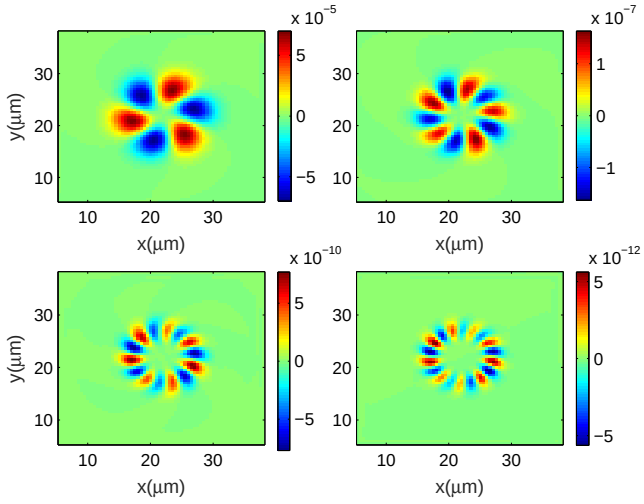

FIG. 4: (color online) Electric field distribution of (a) third, (b) fifth, (c) seventh, and (d) ninth harmonics in $x-y$ plane at $t_1 = 90fs$ and $z_3 = 30\mu$m.

enth and ninth harmonics of precursors at z_3 and t_1 are shown in Fig. 4. According to the number of interwind helices, the azimuthal modes of these harmonics are $l = 3, 5, 7, 9$, respectively. The topological charge of the lth-order harmonic is l, which is expected from the HHG theory [39, 40]. Since the intensity of the lth-order harmonics is inversely proportional to l, the transverse structure of precursors is dominated by the LG_{30}-like mode, as shown in Fig. 1(f). Thus, nonlinear precursors consisting of high-order vortex harmonics appear in the front of the main pulse with a distance that increases during the propagation.

Finally, the root of the nonlinear precursors is discussed based on one-dimensional MB equations with and without RWA. As shown in Fig. 5, in the case without RWA, precursors appear in the front of the 2π SIT soliton, and odd harmonics corresponding to nonlinear precursors emerge in the transmitted spectrum, which

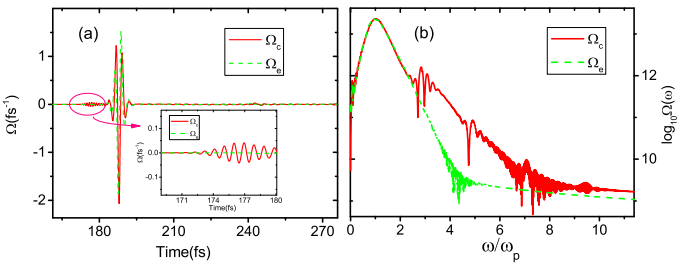

FIG. 5: (color online) The influence of RWA to transmitted fields (a) and spectra (b). The solid and the dashed lines correspond to the case without and with RWA, respectively. The inserts in (a) is the enlarged view of the precursors.

are consistent with the above description of precursors in three-dimensional case. However, in the framework of RWA, both the precursors and the odd-order harmonics disappear. This is because, the carrier induces rapid changes of the refractive index, which in turn can reshape the electric field. When the change of refractive index is proportional to the square of the electric-field value, the two-level atom has a Kerr-medium characteristic [32]. The Kerr nonlinearity, such as intrapulse four-wave mixing and self-phase modulation, could contribute to the occurrence of odd harmonics. The generated odd harmonics propagate faster than the main pulse, forming the preceding nonlinear precursors [18]. While in the framework of RWA, the refractive index barely changes and the nonlinear effect corresponding to ultrafast Bloch oscillation is ignored, which is responsible for the missing of nonlinear precursors in the transmitted spectrum. Therefore, the nonlinear precursors in the transmitted spectrum is generated by carrier effects associated with ultrafast Bloch oscillation.

Our scheme provides a way to manipulate the OAM of a beam by means of nonlinear optics without the requirement of extremely intense light. It also combines the merits of both precursors and high-order vortex harmonics. On one hand, thanks to the advantage of precursors, the obtained high-order vortex harmonics can propagate with the speed of light in vacuum, and instinctively separate from the intense fundamental mode. The obtained high-order vortex precursors can survive the propagation and are resilient to absorption. In addition to be information carriers used in high speed communication, precursors can also be used as optical probes of biological tissues or in underwater communication. On the other hand, since the precursors consist of high-order vortex harmonics, they have potential application in quantum information and communication where multi-dimensional entanglement are required.

This work is supported by the National Natural Science Foundation of China (NNSF, Grant No.11374318 and No. 11374315). C.L. is appreciated to the supports from the 100-Talents Project of Chinese Academy of Sciences and Department of Human Resources and Social Security of China.

[1] J. A. Stratton, *Electromagnetic Theory*, (McGraw-Hill, New York, 1941), 5.18.
[2] A. Sommerfeld, Ann. Phys. **44**, 177 (1914).
[3] L. Brillouin, Ann. Phys. **44**, 203 (1914).
[4] L. Brillouin, *Wave Propagation and Group Velocity* (Academic Press, New York, 1960)
[5] K. E. Oughstun and G. C. Sherman, *Electromagnetic Pulse Propagation in Causal Dielectrics* (Springer-Verlag, Berlin, 1994).
[6] H. A. Lorentz, *The Theory of Electrons* (Dover, New York, 1952).
[7] N. A. Cartwright and K. E. Oughstun, SIAM Rev. **49**, 628 (2007).
[8] H. Jeong and U. L. österberg, Phys. Rev. A **77**, 021803(R) (2008).
[9] H. Jeong and S. Du, Phys. Rev. A **79**, 011802(R) (2009)
[10] B. Macke and B. Segard, Phys. Rev. A **80**, 011803(R) (2009).
[11] W. R. LeFew, S. Venakides, and D. J. Gauthier, Phys. Rev. A **79**, 063842 (2009).
[12] S. Du, P. Kolchin, C. Belthangady, G. Y. Yin, and S. E. Harris, Phys. Rev. Lett. **100**, 183603 (2008).
[13] H. Jeong, A. M. C. Dawes, and D. J. Gauthier, Phys. Rev. Lett. **96**, 143901 (2006).
[14] J. Aaviksoo, J. Kuhl, and K. Ploog, Phys. Rev. A **44**, R5353 (1991).
[15] S.-H. Choi and U. L. österberg, Phys. Rev. Lett. **92**, 193903 (2004).
[16] R. R. Alfano, J. L. Birman, X. Ni, M. Alrubaiee, and B. B. Das, Phys. Rev. Lett. **94**, 239401 (2005).
[17] U. Österberg, D. Andersson and M. Lisak, Opt. Commun. 277, 5 (2007).
[18] D-S. Ding, Y. K. Jiang, W. Zhang, Z.-Y. Zhou, B.-S. Shi, and G.-C. Guo, Phys. Rev. Lett. **114**, 093601 (2015).
[19] R. Marskar and U. L. österberg, Phys. Rev. A **86**, 063826 (2012).
[20] C. L. Palombini and K. E. Oughstun, Opt. Express **18**, 23104 (2010).
[21] J. E. Rothenberg, Opt. Lett. **17**, 1340 (1992).
[22] A. M. Yao and M. J. Padgett, Adv. Opt. Photonics **3**, 161 (2011).
[23] S. Franke-Arnold, L. Allen, and M. Padgett, Laser Photonics Rev. **2**, 299 (2008).
[24] A. Mair, A. Vaziri, G. Weihs, and A. Zeilinger, Nature (London) **412**, 313 (2001).
[25] A. Afanasev, C. E. Carlson, and A. Mukherjee, Phys. Rev. A **88**, 033841 (2013).
[26] A. Picon, A. Benseny, J. Mompart, J. R. V. de Aldana, L. Plaja, G. F. Calvo, and L. Roso, New J. Phys. **12**, 083053 (2010).
[27] A. B. Matsko, A. A. Savchenkov, D. Strekalov, and L. Maleki, Phys. Rev. Lett. **95**, 143904 (2005).
[28] X. Zhang, B. Shen, Y. Shi, X. Wang, L. Zhang, W. Wang, J. Xu, L. Yi, and Z. Xu, Phys. Rev. Lett. **114**, 173901 (2015).
[29] L. Allen, M. W. Beijersbergen, R. J. C. Spreeuw, and J. P. Woerdman, Phys. Rev. A **45**, 8185 (1992).
[30] K. S. Yee, IEEE Trans. Antennas Propag. **14**, 302 (1996).
[31] A. Taflove and M.E. Brodwin, IEEE Trans. Microwave Theory Tech. **23**, 623 (1975).
[32] R. W. Ziolkowski, J. M. Arnold, and D. M. Gogny, Phys. Rev. A **52**, 3082 (1995).
[33] S. Hughes, Phys. Rev. Lett. **81**, 3363 (1998).
[34] X.-Y. Xu, W. Liu, and C. Li, Phys. Rev. A **84**, 033811 (2011).
[35] V. P. Kalosha and J. Herrmann, Phys. Rev. Lett. **83**, 544 (1999).
[36] Y. Niu, S. Gong, and N. Cui, J. Korean Phys. Soc. **60**, 1270 (2012).
[37] Y. Niu, K. Xia, N. Cui, S. Gong, and R. Li, Phys. Rev. A **78**, 063835 (2008).
[38] J. de Lamare, M. Comte, and P. Kupecek, Phys. Rev. A **50**, 3366 (1994).
[39] C. Hernandez-Garcia, A. Picon, J. San Roman, and L. Plaja, Phys. Rev. Lett. **111**, 083602 (2013).
[40] S. Patchkovskii and M. Spanner, Nat. Phys. **8**, 707 (2012).
[41] S. L. McCall and E. L. Hahn, Phys. Rev. 183, 457 (1969).